Ligand Exchange Reactions of Triphospholyl Metal Carbonyl Complexes†

Frank W. Heinemann,‡ Hans Pritzkow,§ Matthias Zeller,‡ and Ulrich Zenneck*,‡

Institut für Anorganische Chemie, Universität Erlangen-Nürnberg, Egerlandstrasse 1, 91058 Erlangen, Germany, and Institut für Anorganische Chemie, Universität Heidelberg, Im Neuenheimer Feld 270, 69120 Heidelberg, Germany

Received December 15, 2000

Utilizing 1-triphenylstannyl-3,5-di(*tert*-butyl)-1,2,4-triphosphole (**2**) as the transfer reagent for the 1,2,4-triphospholyl ligand, the new cobalt dicarbonyl complex (η^5-*t*-$Bu_2C_2P_3$)$(CO)_2$Co (**4**) has been prepared. The reactivity of **4** and that of triphosphacymantrene (η^5-*t*-$Bu_2C_2P_3$)$(CO)_3$Mn (**3**) toward carbonyl exchange have been investigated. When **3** or **4** are photolyzed in the presence of phosphanes the mono- and disubstituted complexes (η^5-*t*-$Bu_2C_2P_3$)(CO)(PR_3)Co (R = Et (**5**), Ph (**6**)) and (η^5-*t*-$Bu_2C_2P_3$)(CO)$(PMe_3)_2$Mn (**7**) are obtained. In the absence of additional ligands, the irradiation of **3** in *n*-hexane results in the formation of the dinuclear *rac* and *meso* complexes {μ[1:1−5-η-*t*-$Bu_2C_2P_3$]$(CO)_2$Mn}$_2$ (**8a** and **8b**). Under thermal conditions the carbonyl ligands of both **3** and **4** are replaced by isonitrile ligands to yield (η^5-*t*-$Bu_2C_2P_3$)$(CN-Cy)_2$Co (**9**), (η^5-*t*-$Bu_2C_2P_3$)(CO)(CN−Cy)Co (**10**), and (η^5-*t*-$Bu_2C_2P_3$)-$(CO)_2$(CN−Cy)Mn (**11**), respectively. The substances have been fully characterized including X-ray structural analysis for the complexes **4**, **6**, **7**, **8a**, **8b**, and **9**. Under both photochemical and thermal conditions the complexes **3** and **4** are much more reactive than their phosphorus-free cyclopentadienyl analogues. In contrast with cymantrene, triphosphacymantrene (**3**) seems to react via an associative pathway.

Introduction

Phosphorus atoms can be incorporated in unsaturated heterocycles to replace CR fragments as isovalent and isolobal building blocks, and this results in the formation of numerous organic and organometallic phosphorus compounds in which the phosphorus atom can often be viewed as a *carbon copy*.[1] One of the most simple examples of organometallic compounds containing a phosphorus heterocyclic π-ligand is phospholyl complexes, the phosphorus analogues of cyclopentadienyl (Cp) compounds. However, in some cases the properties of phospholyl complexes differ significantly from those of their carbacyclic counterparts. Due to the lone pair of the phosphorus atom, which is absent for Cp carbon atoms of course, either the phospholyl ligand can be π-bonded to the metal atom in an η^5-fashion via the delocalized aromatic π-system or it can act as a σ-ligand by utilizing the phosphorus lone pair.[2] Replacing more than one CR fragment of a cyclopentadienyl ligand by phosphorus atoms extends the structural manifold. 1,3-Diphospholyl complexes for example may exhibit an intermediate η^3-bonding type.[3] In recent years a number of complexes have been synthesized containing the 3,5-di(*tert*-butyl)-1,2,4-triphospholyl ligand **1**. Its complex chemistry is dominated by the η^5-complexes,[4−6] but it can also function as a σ-ligand, too.[7] Even a temperature-dependent equilibrium between a π-bonded η^5- and a σ-bonded η^1-nickel complex has been observed.[8]

However, not only does the introduction of phosporus atoms offer novel structural features but the electronic structure of the compounds is influenced significantly as well. Thus hexaphosphamanganocene (η^5-*t*-$Bu_2C_2P_3)_2$-Mn is structurally very closely related to other manganocene derivatives such as Cp^*_2Mn, but the electronic ground state is different when compared to all manganocene derivatives that appeared in the literature.[5]

This strong consequence of the phosphorus atoms on symmetry and energy of the frontier orbitals of the

† Dedicated to Professor Marianne Baudler on the occasion of her 80th birthday.

* Corresponding author. Tel: Int. code +(9131)852-7367. E-mail: zenneck@chemie.uni-erlangen.de.

‡ Universität Erlangen-Nürnberg.

§ Universität Heidelberg.

(1) Dillon, K. B.; Mathey, F.; Nixon, J. F. *Phosphorus, The Carbon Copy*; John Wiley & Sons: Chichester, 1998.

(2) Mathey, F.; Fischer, J.; Nelson, J. H. *Struct. Bonding* **1983**, *55*, 153−201. Mathey, F. *J. Organomet. Chem.* **1994**, *475*, 25−30. Garnowskii, A. D.; Sadimenko, A. P. *Adv. Heterocycl. Chem.* **1999**, *72*, 1−77. Arliguie, T.; Ephritikhine, M.; Lance, M.; Nierlich, M. *J. Organomet. Chem.* **1996**, *524*, 293−297.

(3) Bartsch, R.; Hitchcock, P. B.; Nixon, J. F. *J. Organomet. Chem.* **1989**, *373*, C17−C20. Bartsch, R.; Hitchcock, P. B.; Nixon, J. F. *J. Chem Soc., Chem. Commun.* **1990**, 472−474.

(4) Driess, M.; Hu, D.; Pritzkow, H.; Schäufele, H.; Zenneck, U.; Regitz, M.; Rösch, W. *J. Organomet. Chem.* **1987**, *334*, C35−C38. Callaghan, Ch.; Clentsmith, G. K. B.; Cloke, F. G. N.; Hitchcock, P. B.; Nixon, J. F.; Vickers, D. M. *Organometallics* **1999**, *18*, 793−795.

(5) Clark, T.; Elvers, A.; Heinemann, F. W.; Hennemann, M.; Zeller, M.; Zenneck, U. *Angew. Chem.* **2000**, *112*, 2174−2178. Clark, T.; Elvers, A.; Heinemann, F. W.; Hennemann, M.; Zeller, M.; Zenneck, U. *Angew. Chem., Int. Ed.* **2000**, *39*, 2087−2091.

(6) Bartsch, R.; Hitchcock, P. B.; Madden, T. J.; Meidine, M. F.; Nixon, J. F.; Wang, H. *J. Chem. Soc., Chem. Commun.* **1988**, 1475−1476.

(7) Bartsch, R.; Carmichael, D.; Hitchcock, P. B.; Meidine, M. F.; Nixon, J. F.; Sillet, G. J. D. *J. Chem. Soc., Chem. Commun.* **1988**, 1615−1617. Hitchcock, P. B.; Matos, R. M.; Nixon, J. F. *J. Organomet. Chem.* **1993**, *462*, 319−329.

(8) Heinemann, F. W.; Pritzkow, H.; Zeller, M.; Zenneck, U. *Organometallics* **2000**, *19*, 4283−4288.

10.1021/om001068q CCC: $20.00
Publication on Web 06/01/2001

Scheme 1

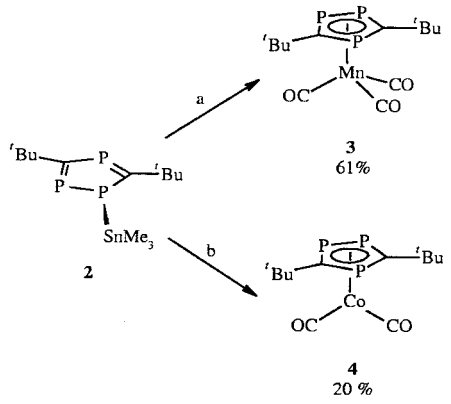

[a] $Br(CO)_5Mn$. [b] $Co_2(CO)_8$.

complexes implies a comparable significant influence on the reactivity of the compounds. However, in the literature there are only few reports on that point.[9] Best candidates for this approach seemed to be half-sandwich compounds such as triphospholylmetal carbonyl complexes. Their Cp analogues undergo a range of clean ligand substitution reactions, which are well described and understood.[10,11] However, most previous attempts to synthesize half-sandwich compounds of the ligand **1** carried out so far failed. There was only one report dealing with triphospholyl rhodium(I) complexes, but no ligand exchange reactions were carried out.[6]

As we found an easy access to triorganylstannyl triphosphole derivatives such as 1-triphenylstannyl-3,5-di(*tert*-butyl)-1,2,4-triphosphole (**2**),[12] which are excellent starting materials for the high-yield transfer of **1**, we started a systematic investigation on the complex chemistry of this phosphorus-rich cyclopentadienyl derivative in detail. This way (η^5-*t*-$Bu_2C_2P_3$)$(CO)_3Mn$ (**3**) is formed in good yield when **2** is reacted with $Br(CO)_5Mn$[5] (Scheme 1). In this contribution we describe the synthesis of the cobalt dicarbonyl complex (η^5-*t*-$Bu_2C_2P_3$)$(CO)_2Co$ (**4**) and the reactivity of (η^5-*t*-$Bu_2C_2P_3$)$(CO)_3Mn$ (**3**) and (η^5-*t*-$Bu_2C_2P_3$)$(CO)_2Co$ (**4**) toward carbonyl substitution reactions.

Results

For investigations on the reactivity of triphospholylmetal carbonyl complexes we needed suitable starting compounds. Therefore we tried to prepare a triphospha derivative of (η^5-Cp)$(CO)_2Co$. Encouraged by the formation of (η^5-*t*-$Bu_2C_2P_3$)$(CO)_3Mn$ (**3**), 1-triphenylstannyl-3,5-di(*tert*-butyl)-1,2,4-triphosphole (**2**) is reacted with an equimolar amount of $Co_2(CO)_8$, and the target complex (η^5-*t*-$Bu_2C_2P_3$)$(CO)_2Co$ (**4**) is formed. Only 20% yield of pure material can be isolated. In contrast to that, ^{31}P NMR spectra of the reaction mixture indicate an initial quantitative formation of **4**. As outlined below, this disagreement might be caused by the high reactivity of **4** toward CO-ligand exchange reactions.

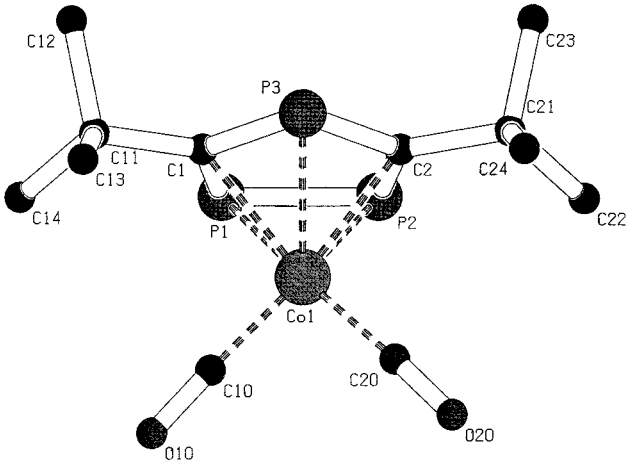

Figure 1. Molecular structure of **4** in the solid state. Hydrogen atoms are omitted for clarity.

As expected for a half-sandwich complex, the ^{31}P NMR spectrum consists of an AB_2 spin system and the signals are separated by only 2.9 ppm. In ^{13}C NMR there is only one signal each for the CO ligands, the ring carbon atoms, and both types of *tert*-butyl carbon atoms.

Despite of its low melting point of ca. −10 °C, X-ray quality crystals of **4** could be obtained from an *n*-hexane solution at about −30 °C. The molecular structure of **4** (Figure 1, Tables 1 and 2) reveals the typical η^5-bonding situation of the *t*-$Bu_2C_2P_3$ ring. The triphospholyl ligand is very close to planar, and both the bond distances and angles show no indications for a distortion.

The plane that is defined by the carbonyl ligands and the mirror plane of the triphospholyl ligand are close to perpendicular to each other. As suggested by the NMR spectra, the *tert*-butyl groups and the adjacent phosphorus atoms are almost equivalent in the solid state. A small deviation is probably caused by packing effects in the solid state. Such an arrangement is found for $Cp^*(CO)_2Co$ as well.[13] The angle between the two carbonyl groups is ca. 91°, which is again in good accordance with the angle of ca. 94° observed for $Cp^*_2(CO)_2Co$.

Photochemical Carbonyl Exchange Reactions of 3 and 4. When **4** is irradiated by visible light in the presence of phosphanes such as PEt_3 or PPh_3, one carbonyl ligand is replaced and the substitution products (η^5-*t*-$Bu_2C_2P_3$)$(CO)(PEt_3)Co$ (**5**) and (η^5-*t*-$Bu_2C_2P_3$)$(CO)(PPh_3)Co$ (**6**) can be isolated in moderate to good yields (Scheme 2). They both exhibit AB_2X ^{31}P NMR spectra; thus no principal structural changes of the triphospholyl cobalt fragment are assumed. As for **4**, the splitting between the A and B signals of **5** is less than 3 ppm, but for **6** a difference of 21 ppm is observed. This indicates a more distinct differentiation of the ring phosphorus atoms of **6**.

5 is a red liquid at room temperature and no crystals could be obtained, whereas **6** is a dark red solid and X-ray suitable crystals can be grown from an *n*-hexane solution at 4 °C. The molecular structure (Figure 2, Tables 1 and 3) confirms the estimated bonding mode with the triphospholyl moiety again being η^5-bonded and

(9) Böhm, D.; Heinemann, F.; Hu, D.; Kummer, S.; Zenneck U. *Collect. Czech. Chem. Commun.* **1997**, *62*, 309−317.
(10) Strohmeier, W.; Müller, F.-J. *Chem. Ber.* **1967**, *100*, 2812−2821. Rehder, D.; Keçeci, A. *Inorg. Chim. Acta* **1985**, *103*, 173−177. Werner, H. *Angew. Chem.* **1983**, *95*, 932−954. Hart-Davis, A. J.; Graham, W. A. G. *Inorg. Chem.* **1970**, *9*, 2658−2663.
(11) Yamamoto, Y.; Mise, T.; Yamazaki, H. *Bull. Chem. Soc. Jpn.* **1978**, *51*, 2743−2744.
(12) Elvers, A.; Heinemann, F. W.; Wrackmeyer, B.; Zenneck, U. *Chem. Eur. J.* **1999**, *5*, 3143−3153.
(13) Byers, L. R.; Dahl, L. F. *Inorg. Chem.* **1980**, *2*, 277−284.

Table 1. Crystal Data and Structure Refinement of 4 and 6

	4	6
empirical formula	$C_{12}H_{18}CoP_3$	$C_{29}H_{33}CoOP_4$
fw	346.10	580.3
solvent	*n*-hexane	*n*-hexane
cryst habit	reddish brown plate	dark red block
cryst size	0.50 × 0.40 × 0.18 mm	0.60 × 0.42 × 0.20 mm
temperature	200(2) K	298(2) K
cryst syst	triclinic	monoclinic
space group	*P*1	$P2_1/n$
unit cell dimens	$a = 6.396(2)$ Å	$a = 12.133(2)$ Å
	$b = 9.787(2)$ Å	$b = 14.947(3)$ Å
	$c = 13.472(3)$ Å	$c = 16.193(3)$ Å
	$\alpha = 96.94(2)°$	$\alpha = 90°$
	$\beta = 98.87(3)°$	$\beta = 91.03(3)°$
	$\gamma = 107.91(2)°$	$\gamma = 90°$
volume	780.1(3) Å^3	2936(1) Å^3
Z	2	4
density (calcd)	1.474 g/cm^3	1.313 g/cm^3
F(000)	356	1208
abs coeff	1.398 mm^{-1}	0.822 mm^{-1}
θ range for data collection	2.22−27.00°	1.85−27.00°
index ranges	$-8 \le h \le 1$,	$-15 \le h \le 15$,
	$-12 \le k \le 12$,	$-1 \le k \le 19$,
	$-17 \le l \le 17$	$-1 \le l \le 20$
no. of reflns collected	4242	7650
no. of ind reflns	3335 [*R*(int) = 0.0332]	6413 [*R*(int) = 0.0376]
no. of reflns with $I > 2\sigma(I)$	2421	3866
abs corr	ψ-scan	no
max. and min. transm	0.4611 and 0.3466	
refinement method	full matrix least-squares on F^2	
no. of data/restraints/params	3335/0/217	6413/0/415
goodness-of-fit on F^2	1.033	0.852
final *R* indices [$I > 2\sigma(I)$]	R1 = 0.0598, wR2 = 0.1473	R1 = 0.0407, wR2 = 0.0892
R indices (all data)	R1 = 0.0891, wR2 = 0.1671	R1 = 0.0767, wR2 = 0.0982
largest diff peak and hole	0.873 and −0.737 e Å^{-3}	0.346 and −0.354 e Å^{-3}

Table 2. Selected Bond Lengths (Å) and Angles (deg) for 4

Co−C(10)	1.747(6)
Co−C(20)	1.759(5)
P(1)−P(2)	2.099(2)
P(2)−C(2)	1.781(6)
P(3)−C(1)	1.759(5)
P(3)−C(2)	1.773(5)
P(1)−C(1)	1.796(5)
C(10)−O(10)	1.145(7)
C(20)−O(20)	1.142(6)
C(10)−Co−C(20)	91.2(3)
Co−C(10)−O(10)	178.6 (6)
Co−C(20)−O(20)	177.9 (5)
P(1)−C(1)−P(3)	122.3(3)
C(1)−P(3)−C(2)	96.9(2)
P(3)−C(2)−P(2)	123.3(3)
C(2)−P(2)−P(1)	98.24(17)
P(2)−P(1)−C(1)	99.24(16)

Scheme 2

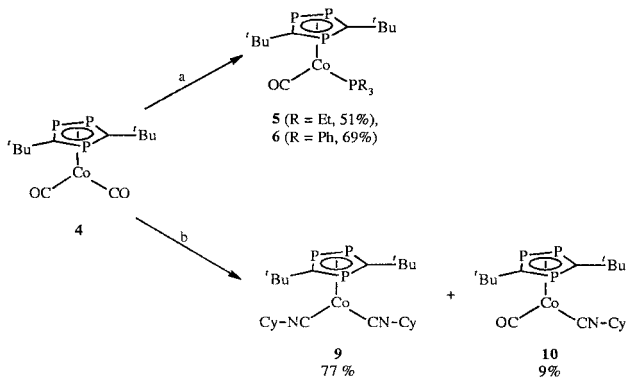

[a] PR_3, *hν*, 15 min. [b] 2 equiv of CN−Cy, −60 °C → rt.

the angle built up by the two co-ligands being 90.7°. In contrast with **4**, the orientation of the co-ligands is now in parallel with the vertical mirror plane of the π-ligand and the bulky triphenylphosphane is situated in a trans position with respect to the single phosphorus atom P3. This position grants the maximum of space available for this ligand. Most probably this conformation represents the thermodynamic favorable situation in solution as well; thus independent from a potential high barrier of the ring rotation of the heterocycle, the differing trans effects of CO and PPh_3 ligands might explain the differences of the chemical shifts of the ^{31}P ring nuclei of **6**.

When the manganese complex (η^5-*t*-$Bu_2C_2P_3$)$(CO)_3Mn$ (**3**) is irradiated in the presence of excess trimethylphosphane, two carbonyl ligands are readily displaced to form (η^5-*t*-$Bu_2C_2P_3$)$(CO)(PMe_3)_2Mn$ (**7**) in 74% yield (Scheme 3). At room temperature the NMR spectra of **7** exhibit very broad lines. A coalescence phenomenon was considered, and thus a variable-temperature NMR experiment was applied. At −60 °C the ^{31}P NMR spectrum of **7** forms an ABCDE spin system with all phosphorus atoms being different (Figure 3). The signals of the two adjacent phosphorus atoms a and b are separated by 52 ppm and exhibit a coupling constant $^1J(^{31}P,^{31}P)$ of 432 Hz, and the two trimethylphosphane groups are discriminated likewise and separated by 5.6 ppm. From the ^{31}P NMR coalescence temperatures of 22 ± 5 °C for the adjacent ring phosphorus atoms and 50 ± 5 °C for the phosphane groups, the activation energy for the rotation of the triphospholyl ring can be calculated to be 53.5 kJ mol^{-1}.[14]

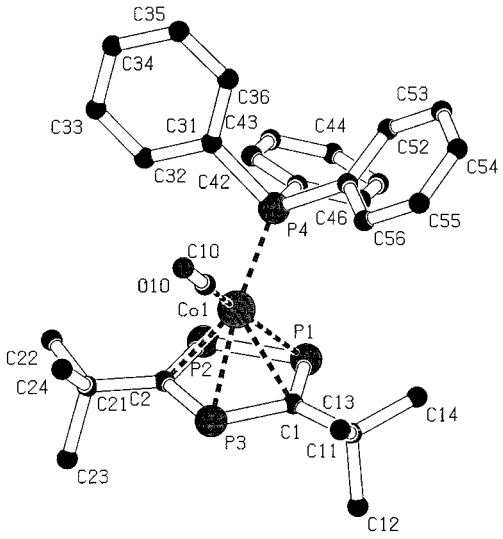

Figure 2. Molecular structure of **6** in the solid state. Hydrogen atoms are omitted for clarity.

Table 3. Selected Bond Lengths (Å) and Angles (deg) for 6

Co−C(10)	1.725(4)
Co−P(4)	2.1760(10)
P(1)−P(2)	2.1620(14)
P(2)−C(2)	1.744(3)
P(3)−C(1)	1.760(3)
P(3)−C(2)	1.773(3)
P(1)−C(1)	1.758(3)
C(10)−O(10)	1.153(4)
C(10)−Co−P(4)	90.72(11)
Co−C(10)−O(10)	179.0(4)
P(1)−C(1)−P(3)	120.54(17)
C(1)−P(3)−C(2)	99.77(14)
P(3)−C(2)−P(2)	121.95(18)
C(2)−P(2)−P(1)	98.14(11)
P(2)−P(1)−C(1)	99.59(11)

Scheme 3

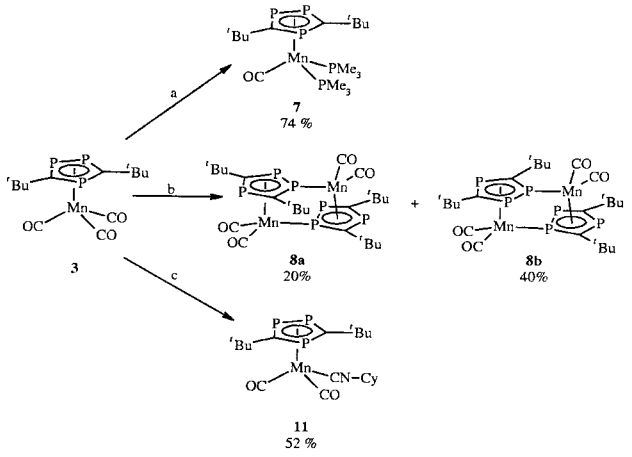

[a] PMe_3, *hν*, 15 min. [b] *hν*, 15 min. [c] Cy−NC, −70 °C, 3 h.

In accordance with the ^{31}P NMR observations, the ^{13}C NMR spectrum of **7** consists of separate lines for all sorts of carbon atoms at low temperature. The signals of the ring carbon atoms are separated by 4.8 ppm and exhibit $^1J(^{13}C,^{31}P)$ values, which range from 70 to 90 Hz, whereas the ^{13}C signal of the carbonyl ligand

(14) Günther, H. *NMR−Spektroskopie, Eine Einführung in die Protonenresonanzspektroskopie und ihre Anwendungen in der Chemie*, 2nd corrected ed.; Georg Thieme Verlag: Stuttgart, New York, 1983.

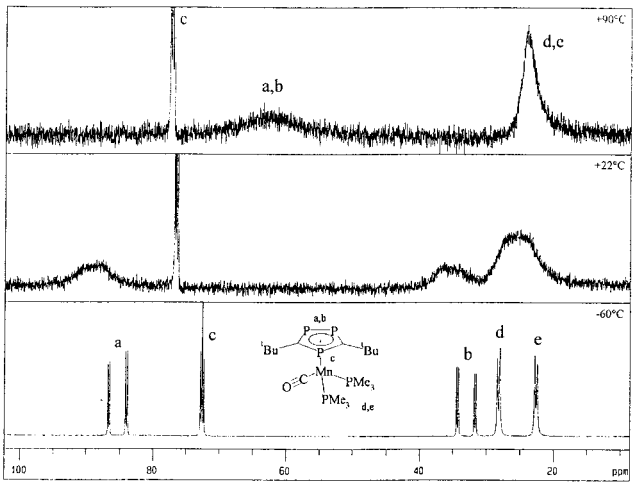

Figure 3. Temperature-dependent $^{31}P\{^1H\}$ NMR spectra (161.7 MHz, [D_8] toluene) of **7**.

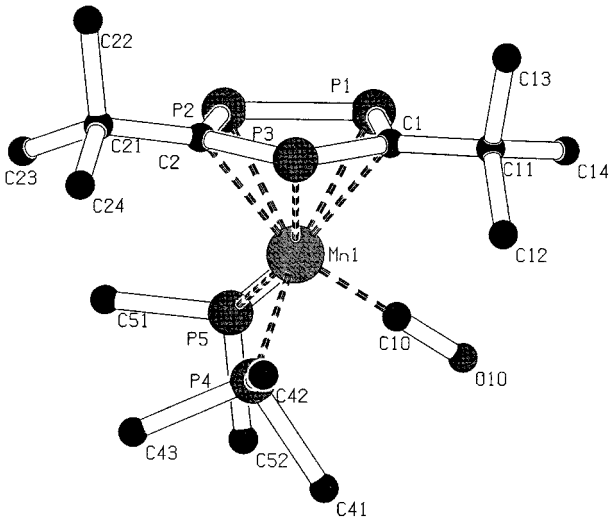

Figure 4. Molecular structure of **7** in the solid state. Hydrogen atoms are omitted for clarity.

appears as a triplet, which is attributed to the interaction with the two phosphorus atoms of the PMe_3 ligands. To explain the low-temperature ^{31}P and ^{13}C NMR results, the molecule is assumed to be rigid and of C_1 symmetry. The vertical mirror plane of ligand **1** must be extinguished by the orientation of the co-ligands.

This assumption was corroborated by an X-ray diffraction study of **7** (Figure 4, Tables 4 and 5). The molecular structure in the solid state reveals the unsymmetrical arrangement of the two PMe_3 ligands. When considering the comparable space-filling properties of the *tert*-butyl groups and the PMe_3 ligands, a sterical overcrowded situation is evident. The central carbon atom C11 of the *tert*-butyl moiety, which is not influenced by the two phosphane groups, is located close to the plane built up by the triphospholyl ring, whereas corresponding C21 is displaced by 27.9(3) pm. Additionally the manganese carbon bond Mn−C1 is 5.5 pm shorter than Mn−C2.

The triphospholyl complexes are ligands themselves. Due to its phosphorus lone pairs **3** reacts with (thf)$(CO)_5Cr$ to yield the binuclear manganese chromium complex $\{\mu[1{:}1{-}5{-}\eta{-}t{-}Bu_2C_2P_3]\}\{(CO)_5Cr\}\{(CO)_3Mn\}$.[5] Therefore photolysis of $(\eta^5{-}t{-}Bu_2C_2P_3)(CO)_3Mn$ (**3**) without addition of further ligands was attempted. Within

Table 4. Crystal Data and Structure Refinement of 7 and 9

	7	9
empirical formula	$C_{17}H_{36}MnOP_5$	$C_{24}H_{40}CON_2P_3$
fw	466.28	508.42
solvent	*n*-hexane	*n*-hexane
cryst habit	orange rhombohedron	part of dark red needle
cryst size	0.7 × 0.4 × 0.25 mm	0.36 × 0.11 × 0.06 mm
temperature	220(2) K	173(2) K
cryst syst	monoclinic	rhombohedral
space group	$P2_1/c$	$R3c$
unit cell dimens	a = 12.264(1) Å	a = 33.6732(12) Å
	b = 10.444(1) Å	b = 33.6732(12) Å
	c = 18.505(2) Å	c = 12.0325(8) Å
	α = 90°	α = 90°
	β = 94.66(1)°	β = 90°
	γ = 90°	γ = 120°
volume	2362.4(4) Å^3	11815.6(8) Å^3
Z	4	18
density (calcd)	1.311 g/cm^3	1.286 g/cm^3
F(000)	984	4860
abs coeff	0.901 mm^{-1}	0.850 mm^{-1}
θ range for data collection	2.21−27.00°	1.21−27.86°
index ranges	$-1 \le h \le 15$,	$0 \le h \le 20$,
	$-13 \le k \le 1$,	$0 \le k \le 13$,
	$-23 \le l \le 23$	$0 \le l \le 22$
no. of reflns collected	6538	26 971
no. of ind reflns	5160 [R(int) = 0.0214]	5982 [R(int) = 0.050]
no. of reflns with $I > 2\sigma(I)$	4383	4993
abs corr	ψ-scan	ψ-scan
max. and min. transm	0.3643 and 0.3238	0.928 and 0.711
refinement method	full matrix least squares on F^2	
no. of data/restraints/params	5160/0/325	5982/1/431
goodness-of-fit on F^2	1.048	0.927
final R indices [$I>2\sigma(I)$]	R1 = 0.0290, wR2 = 0.0670	R1 = 0.0325, wR2 = 0.0576
R indices (all data)	R1 = 0.0384, wR2 = 0.0712	R1 = 0.0466, wR2 = 0.0609
largest diff peak and hole	0.269 and −0.373 e Å^{-3}	0.394 and −0.203 e Å^{-3}

Table 5. Selected Bond Lengths (Å) and Angles (deg) for 7

Mn−C(10)	1.762(2)
Mn−P(4)	2.2785(5)
Mn−P(5)	2.2643(6)
C(10)−O(10)	116.3(2)
P(1)−P(2)	2.1133(7)
P(2)−C(2)	1.7555(17)
P(3)−C(1)	1.7490(18)
P(1)−C(1)	1.7668(18)
P(3)−C(2)	1.7647(18)
Mn−C(10)−O(10)	179.0(2)
P(1)−C(1)−P(3)	121.86(10)
C(1)−P(3)−C(2)	99.64(12)
P(3)−C(2)−P(2)	119.81(10)
C(2)−P(2)−P(1)	100.66(6)
P(2)−P(1)−C(1)	98.00(6)
C(10)−Mn−P(4)	88.45(6)
C(10)−Mn−P(5)	85.19(7)
P(4)−Mn−P(5)	94.53(2)

15 min 1 equiv of carbon monoxide is removed and replaced by a phosphorus atom of a second triphospholyl complex to result in the formation of homobinuclear species. Because of σ-coordination of a manganese atom by one of the neighboring phosphorus atoms of the triphospholyl ring, the vertical mirror plane of the π-ligand is lost again and the diastereomeric *rac* and *meso* complexes **8a** and **8b**, $\{\mu[1{:}1{-}5{-}\eta{-}t{-}Bu_2C_2P_3](CO)_2{-}Mn\}_2$, are isolated (Scheme 3).

Crystals suitable for X-ray analysis of both complexes can be isolated after chromatography of the reaction mixture. Slow solvent evaporation of a $CDCl_3$ solution yields crystals of the *meso* compound (**8b**). It crystallizes in the triclinic space group $P\bar{1}$ with two symmetrically independent molecules in the unit cell. Both are located on a crystallographic inversion center. Crystals of the

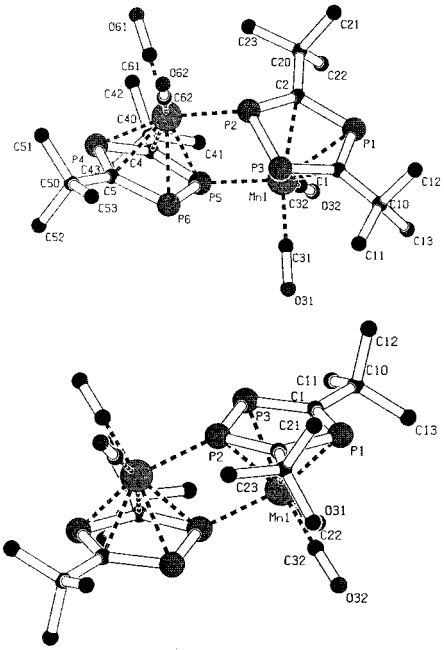

Figure 5. Molecular structures of **8a** (top) and **8b** (bottom) in the solid state. Hydrogen atoms are omitted for clarity.

rac isomer (**8a**) were obtained from *n*-hexane at 4 °C. The space group is $P2_1/n$. Both enantiomers are present in the unit cell. They are close to C_2 symmetric (Figure 5, Tables 6, 7, and 8).

The main difference between the two diastereomers is the orientation of the two metal−phosphorus σ-bonds. In the case of the *rac* isomer **8a**, both bridging P atoms P2 and P5 point to the same side of the molecule, whereas in the case of the *meso* isomer they are

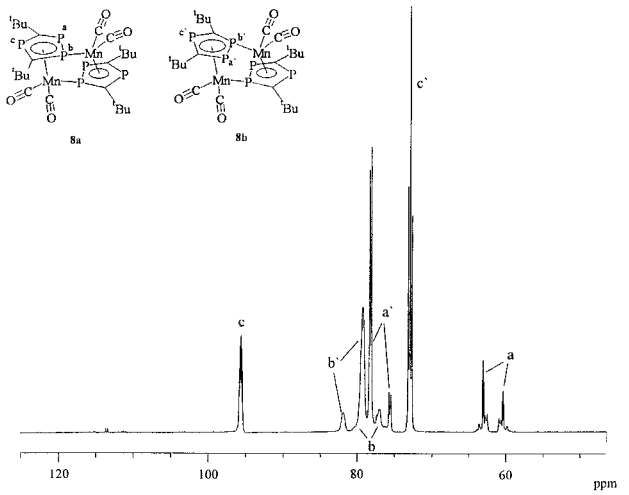

Figure 6. $^{31}P\{^1H\}$ NMR spectrum (161.7 MHz, $CDCl_3$, 23 °C) of a mixture of **8a** and **8b**.

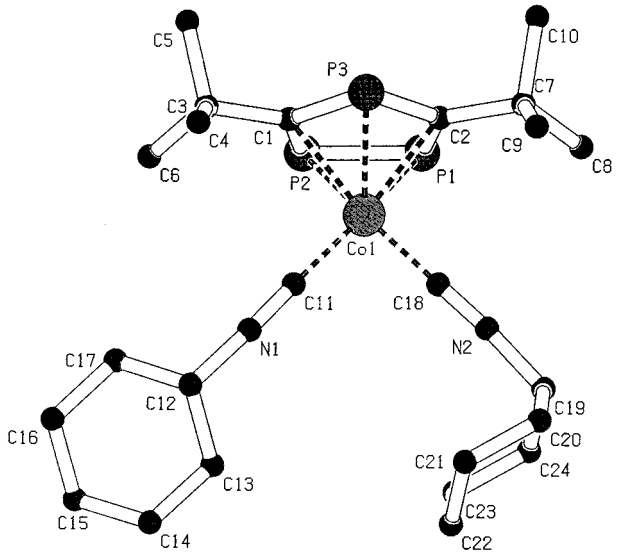

Figure 7. Molecular structure of **9** in the solid state. Hydrogen atoms are omitted for clarity.

orientated to opposite sides. On the other hand the bond lengths and angles within the triphospholyl ligands of **8a** and **8b** are almost identical. The bond angles around the manganese atom and the σ-bonded phosphorus atoms differ by a maximum of 6°, and the distance between the manganese and the σ-bonded phosphorus atoms are 2.271(2) Å for the *rac* and 2.256(1) Å for the *meso* isomer. These values are in good agreement with the mean value of 2.271 Å found for the Mn−P distances in **7**.

Not only the structural but also the spectroscopic properties of **8a** and **8b** point to their close relation. Solutions of mixture of **8a** and **8b** exhibit only two carbonyl stretching modes at 1962 und 1930 cm^{-1}. This is indicative for electronically almost identical manganese centers.

In contrast to that, **8a** and **8b** exhibit very different NMR properties. Due to strong P−P coupling, the ^{31}P NMR spectra are influenced most and (Figure 6) two independent sets of signals are observed. The major *meso* isomer **8b** generates an $[ABC]_2$ spin system with no significant interaction between the two halves of the molecule. The $^1J(^{31}P,^{31}P)$ coupling constant of the two adjacent phosphorus atoms A and B is 424 Hz, and the $^2J(^{31}P,^{31}P)$ values are about 40 Hz; thus the ^{31}P NMR parameters of **8b** resemble those of **3** at low temperature. Caused by the nuclear quadrupole moment of manganese, the signal of the σ-metal-bonded phosphorus atom is severely broadened.

The minor isomer **8a** behaves completely different in ^{31}P NMR, as it shows a strong interaction between the two triphospholyl rings. Despite the fact that one of its signals is hidden by a signal of **8b**, the spin system is assumed to be of the type AA′XX′YY′. As there is no analytical solution for this spin system,[15] the coupling constants could not yet be determined. Nevertheless, at least one of the coupling constants $J(^{31}P,^{31}P)$ between the two triphospholyl rings must be in the same range as those within the five-membered rings. Because of the quadrupole moment of the manganese atom, a coupling mechanism along σ- and π-bonds of the metal is very unlikely. ^{31}P coupling constants of 40 Hz or more between phosphorus atoms, which are not connected by a chemical bond, point to a direct lone pair interaction of the involved phosphorus atoms.[16] An interaction of the π-electrons is possible in both **8a** and **8b**, but only for the *rac* isomer **8a** are the lone pairs of P3 and P6, which belong to different rings, directing toward each other (Figure 5). The distance between P3 and P6 of **8a** is about 3.28 Å, which is less than twice the van der Waals radius of phosphorus atoms (3.6 Å).[17]

Thermal Carbonyl Exchange Reactions of 3 and 4. As the photochemical carbonyl exchange reactions of **3** and **4** are surprisingly fast, a thermal reaction pathway seemed to be possible as well. When **4** is allowed to react with phosphanes at room temperature in solution, a slow replacement of one CO ligand is observed. After one day there are only small amounts of a substitution product observable in the IR. In contrast to that, **4** reacts under the same conditions readily with cyclohexylisonitrile and no irradiation or heating is needed. Using 2 equiv of isonitrile leads to the formation of two products (Scheme 2). The main one is (η^5-*t*-$Bu_2C_2P_3$)$(CN-Cy)_2Co$ (**9**), which is isolated in 77% yield. The spectroscopic features resemble closely those found for the dicarbonyl complex **4**, indicating no principal structural changes upon substitution of the σ-ligands.

9 forms crystals of two polymorphous forms, dark red needles and yellow to brown thin plates, and both have been analyzed by X-ray crystallography. The thin plates were of low quality, but red needles allowed a precise analysis (Figure 7, Tables 4 and 9). The molecular structures of **9** in the solid state represent different conformers; thus only the better set of data will be discussed.[18] The triphospholyl moiety is η^5-bonded and the isonitrile ligands are arranged in the same manner

(15) Lustig, E.; Duy, N.; Diehl, P.; Kellerhals, H. *J. Chem. Phys.* **1968**, *48*, 5001−5007.

(16) Baudler, M.; Düster, D.; Heumüller, R. In *Phosphorus-31-P NMR Spectral Properties in Compound Characterization and Structural Analysis*; Quin, L. D., Verkade, J. G., Eds.; VCH: New York, 1994; pp 81−91. Baudler M.; Hahn, J.; Arndt, V.; Knoll, B.; Kazmierczak, K.; Darr, E. *Z. Anorg. Allg. Chem.* **1986**, *538*, 7−20. Baudler, M.; Reuschenbach, G.; Hahn, J. *Chem. Ber.* **1983**, *116*, 847−855.

(17) Bondi, A. *J. Chem. Phys.* **1964**, *68*, 441.

(18) The only main difference between the two structures of **9** is the orientation of the cyclohexyl rings, which are rotated by ca. 90°.

Table 6. Crystal Data and Structure Refinement of 8a and 8b[a]

	8a	8b
empirical formula	$C_{24}H_{36}Mn_2O_4P_6$	$C_{24}H_{36}Mn_2O_4P_6$
fw	684.23	684.23
solvent	*n*-hexane	$CDCl_3$
cryst habit	red rhombohedron	red block
cryst size	0.55 × 0.15 × 0.10 mm	0.90 × 0.50 × 0.30 mm
temperature	220(2) K	294(2) K
cryst syst	monoclinic	triclinic
space group	$P2(1)/n$	$P\bar{1}$
unit cell dimens	$a = 10.606(2)$ Å	$a = 11.087(1)$ Å
	$b = 9.898(2)$ Å	$b = 12.127(1)$ Å
	$c = 29.882(6)$ Å	$c = 12.226(1)$ Å
	$\alpha = 90°$	$\alpha = 89.20(1)°$
	$\beta = 96.31(2)°$	$\beta = 83.61(1)°$
	$\gamma = 90°$	$\gamma = 72.36(1)°$
volume	3118.0(11) Å^3	1556.4(2) Å^3
Z	4	2
density (calcd)	1.458 g/cm^3	1.460 g/cm^3
$F(000)$	1408	704
abs coeff	1.145 mm^{-1}	1.147 mm^{-1}
θ range for data collection	1.98−25.00°	1.65−29.00°
index ranges	$-1 \le h \le 12$,	$-15 \le h \le 1$,
	$-1 \le k \le 11$,	$-16 \le k \le 16$,
	$-35 \le l \le 35$	$-16 \le l \le 16$
no. of reflns collected	7271	9519
no. of ind reflns	5504 [R(int) = 0.0436]	8290 [R(int) = 0.0155]
no. of reflns with $I > 2\sigma(I)$	3574	6777
abs corr	ψ-scan	
max. and min. transm	0.4570 and 0.3967	0.2671 and 0.3295
refinement method	full matrix least squares on F^2	
no. of data/restraints/params	5504/0/433	8290/0/465
goodness-of-fit on F^2	1.016	1.053
final R indices [$I>2\sigma(I)$]	R1 = 0.0497, wR2 = 0.0899	R1 = 0.0338, wR2 = 0.0832
R indices (all data)	R1 = 0.0958, wR2 = 0.1063	R1 = 0.0451, wR2 = 0.0892
largest diff peak and hole	0.432 and −0.493 e Å^{-3}	0.370 and −0.351 e Å^{-3}

[a] The unit cell of **8b** contains two symmetrically independent molecules, which are both located on a crystallographic inversion center. A disorder is observed in one of the *tert*-butyl groups in **8b**, where two alternative sites were refined, giving a site occupancy of the major component of 77.0(7)% for C21, C22, C23. Further information is available in the Supporting Information.

as the CO ligands of dicarbonyl complex **4**. As expected a plane is built up by the CNC−Co−CNC part of the complex, which is orientated almost perpendicular to the plane of the triphospholyl ring. This indicates a preferred ligand arrangement for this type of complex in the absence of sterical overcrowded situations. The coordinated isonitrile ligands form almost linear Co−C−N−C units, with Co−C−N and C−N−C bond angles of about 178−179°.

The second reaction product is the monosubstitution compound (η^5-*t*-$Bu_2C_2P_3$)(CO)(CNCy)Co (**10**), which is formed in about 9% yield. This compound is a red to tan liquid at room temperature. Since no crystals could be obtained, **10** was characterized by spectroscopic methods. The FD$^+$ mass spectrum shows only the molecule peak, and the IR spectrum exhibits strong bands at 1978 and 2135 cm^{-1}, attributed to the CO and CN stretching vibrations, respectively. The ^{31}P NMR spectrum consists of an AB_2 spin system with the two groups of signals separated by less than 1 ppm. The identity of **10** is further established by the ^{13}C NMR data, which are also in accord with a structure similar to those found for **4** and **9**. Assuming the same preferred orientation of the co-ligands as for **4** and **9**, the vertical mirror plane of the triphospholyl ligand would be eliminated. To explain the NMR spectroscopic properties of **10**, the triphospholyl ligand is assumed to rotate free within the NMR time scale.

Even triphosphacymantrene **3** shows a remarkable reactivity toward thermally initiated ligand exchange. When it is reacted for 3 h with an excess of cyclohexylisonitrile at 70 °C, no triphosphacymantrene **3** is left over. After chromatographic workup, the monosubstituted complex (η^5-*t*-$Bu_2C_2P_3$)(CN−Cy)$(CO)_2$Mn (**11**) is isolated in 52% yield as an orange to red liquid.

The FD$^+$ mass spectrum of **11** shows only the molecule peak, and the solution IR spectrum exhibits one absorption at 2118 cm^{-1}, which can be attributed to the isonitrile ligand, and two ν(CO) bands at 1968 and 1927 cm^{-1}. The ^{1}H NMR spectrum shows only one signal for the *tert*-butyl groups. Likewise, the ^{31}P NMR spectrum of **11** supplies little information, as the nuclei are isochronic, and only one sharp signal results. Due to the proximity of the ^{31}P signals, the ^{13}C NMR signals of the triphospholyl ligand represent the X-parts of AB_2X spin systems (A, B = ^{31}P, X = ^{13}C). As a result, each of the signals exhibits an unsymmetric coupling pattern and consists of eight lines.[19] Due to the lack of information from the ^{31}P spectrum, no unambiguous ascertainment of the coupling constants is possible.

Mechanistic Aspects. The reactivity of **3** and **4** toward CO ligand exchange is remarkably high, and this is true for the photochemically and thermally initiated reactions. To compare the triphospholyl complexes with their parent cyclopentadienyl compounds, the cobalt and manganese complexes have to be taken separately.

Ligand exchange reactions of cymantrene derivatives do not occur under thermal conditions, and photochemi-

(19) Emsley, J. W.; Feeney, J.; Suthcliffe, L. H. *High-Resolution Nuclear Magnetic Resonance*, 1st ed., 2nd impression; Pergamon Press: Oxford: 1967; Vol. 1, pp 365−370.

Table 7. Selected Bond Lengths (Å) and Angels (deg) for 8a[a]

Mn(1)−C(31)	1.789(6)
Mn(1)−C(32)	1.805(5)
Mn(2)−C(61)	1.801(6)
Mn(2)−C(62)	1.792(5)
Mn(1)−P(5)	2.2704(15)
Mn(2)−P(2)	2.2715(15)
C(31)−O(31)	1.154(6)
C(32)−O(32)	1.154(6)
C(61)−O(61)	1.157(6)
C(62)−O(62)	1.150(6)
P(2)−P(3)	2.1315(19)
P(5)−P(6)	2.1280(18)
P(2)−C(2)	1.755(5)
P(5)−C(4)	1.764(5)
P(3)−C(1)	1.755(5)
P(6)−C(5)	1.765(5)
P(1)−C(1)	1.758(5)
P(4)−C(5)	1.752(5)
P(1)−C(2)	1.778(5)
P(4)−C(4)	1.768(5)
Mn(1)−C(31)−O(31)	178.9(5)
Mn(1)−C(32)−O(32)	176.0(5)
P(2)−Mn(2)−C(62)	90.03(16)
P(2)−Mn(2)−C(61)	102.09(16)
C(31)−Mn(1)−C(32)	89.3(2)
P(3)−P(2)−Mn(2)	111.50(7)
C(2)−P(2)−Mn(2)	138.64(17)
P(1)−C(1)−P(3)	122.7(3)
C(1)−P(3)−P(2)	96.93(18)
P(3)−P(2)−C(2)	102.02(17)
P(2)−C(2)−P(1)	118.3(3)
C(2)−P(1)−C(1)	100.0(2)

[a] The data of only half of the molecule are given. The second half is almost isostructural. Further information is available in the Supporting Information.

Table 8. Selected Bond Lengths (Å) and Angles (deg) for 8b[a]

Mn(1)−C(31)	1.793(2)
Mn(1)−C(32)	1.804(2)
Mn(1)−P(2$^{\#1}$)	2.256(1)
C(31)−O(31)	1.150(3)
C(32)−O(32)	1.141(3)
P(2)−P(3)	2.121(1)
P(2)−C(2)	1.755(2)
P(3)−C(1)	1.766(2)
P(1)−C(2)	1.778(2)
P(1)−C(1)	1.756(2)
P(2)−P(2$^{\#1}$)	2.746(1)
P(2)−P(3$^{\#1}$)	3.440(1)
Mn(1)−C(31)−O(31)	176.8(2)
Mn(1)−C(32)−O(32)	177.3(2)
C(31)−Mn(1)−C(32)	87.41(10)
P(2$^{\#1}$)−Mn(1)−C(31)	96.01(7)
P(2$^{\#1}$)−Mn(1)−C(32)	94.65(7)
P(1)−C(1)−P(3)	122.5 (11)
C(1)−P(3)−P(2)	96.88(7)
P(3)−P(2)−C(2)	102.2(7)
P(2)−C(2)−P(1)	118.33(11)
C(2)−P(1)−C(1)	99.87(9)
P(3)−P(2)−Mn(1$^{\#1}$)	115.92(3)
C(2)−P(2)−Mn(1$^{\#1}$)	134.01(7)

[a] Only the data of one of the two symmetrically independent molecules are given. # indicates symmetry equivalent atoms. Symmetry transformations used to generate equivalent atoms: $^{\#1}$: $-x+1, y+2, -z$, $^{\#2}$: $-x+1, -y+3, -z-1$. Further information is available in the Supporting Information.

cal activation is the method of choice. Concerning the mechanism, the initial and rate-determining step is the photochemical abstraction of one carbonyl ligand. The resulting 16-VE intermediate immediately forms a solvent complex, and the solvent is replaced again by a ligand or the deliberated free carbon monoxide[20−22] (Scheme 4). In the case of short irradiation times, monosubstituted complexes are isolated exclusively, but after prolonged photolysis (≥100 min) the primary products react further and disubstituted complexes are formed.[23]

Table 9. Selected Bond Lengths (Å) and Angles (deg) for 9

Co−C(11)	1.814(3)
Co−C(18)	1.800(3)
P(1)−P(2)	2.1005(10)
P(2)−C(1)	1.785(3)
P(3)−C(1)	1.768(3)
P(3)−C(2)	1.763(3)
P(1)−C(2)	1.789(3)
C(11)−N(1)	1.164(3)
C(18)−N(2)	1.157(3)
C(11)−Co−C(18)	90.61(11)
Co−C(11)−N(1)	178.3(2)
Co−C(18)−N(2)	178.6(3)
P(1)−C(2)−P(3)	122.63(15)
C(2)−P(3)−C(1)	97.00(12)
P(3)−C(1)−P(2)	122.71(15)
C(1)−P(2)−P(1)	98.70(9)
P(2)−P(1)−C(2)	98.81(9)

Scheme 4

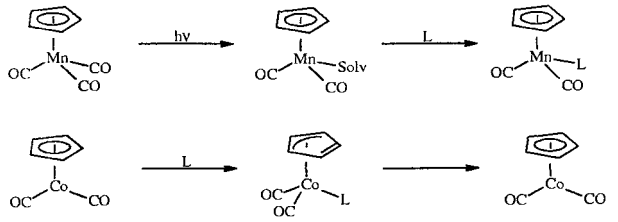

$CpCo(CO)_2$ follows a different mechanism. The CO exchange is generally thermally initiated, and the kinetics of the reaction are first-order according to both the starting complex and the added ligand. An associative reaction pathway is thus assumed. The intermediate species $CpCo(CO)_2L$ avoids exceeding 18 VE by a ring slippage of the Cp ligand, and the substitution product is formed subsequently by the loss of one carbonyl ligand. In most cases CpCo(CO)L complexes are formed.[24,25]

As already outlined, the ligand exchange reactions of **3** and **4** are much more rapid than those of their parent Cp complexes. When irradiated with a 125 W high-pressure Hg vapor lamp in the presence of phosphanes, the reactions of **3** and **4** are completed after 10−15 min. As we are using Duran glassware, the UV part of the lamp spectrum is absorbed. Under these conditions, the cobalt complex **4** forms monosubstituted products, but

(20) Teixeira, G.; Avilés, T.; Dias, A. R.; Pina, F. *J. Organomet. Chem*. **1988**, *353*, 83−91.

(21) Herberhold, M.; Kremnitz, W.; Trampisch, H.; Hitam, R. B.; West, A. J.; Taylor, D. J. *J. Chem. Soc., Dalton Trans.* **1982**, 1261−1273.

(22) Creaven, B. S.; Dixon, A. J.; Kelly, J. M.; Long, C.; Poliakoff, M. *Organometallics* **1987**, *6*, 2600−2605.

(23) The reaction times for total conversions are between ca. 100 min ($(\eta^5$-Cp′$)(CO)_3$Mn with PPh_3, 90 W medium-pressure Hg vapor lamp)[20] and ca. 5 h ($(\eta^5$-Cp$)(CO)_3$Mn with PEt_3, 200 W medium-pressure Hg vapor lamp).[21]

(24) Rerek, M. E.; Basalo, F. *Organometallics* **1982**, *2*, 372−376.

(25) For adequate reaction rates normally elevated temperatures are needed. The ligand substitution reactions of $(\eta^5$-Cp$)(CO)_2$Co are faster than those of Cp* derivatives, which can be explained by the higher sterical demands of Cp*. In addition the cone angle of the incoming ligand affects the reaction rates as well.[24]

triphosphacymantrene **3** yields the disubstituted complex **7** selectively. Even after this short reaction time there are no detectable traces of a manganese monophosphane complex. Therefore, the reaction rate of **3** seems to be increased by several orders of magnitude when compared with carbacyclic cymantrenes.[23]

It has to be stated that the enhancement of the reaction rate does not depend directly on the number of phosphorus atoms in the five-membered ring ligand. Monophosphacymantrene derivatives, for example, are less reactive than their carbacyclic analogues. If they are irradiated in the presence of phosphanes, only monosubstituted complexes are formed even after one day reaction time. Only trimethyl phosphite allows the formation of small amounts of the disubstituted product.[26]

As a consequence, the difference in the photochemical reactivity between cymantrene and triphosphacymantrene is unexpected. **3** exhibits only a slightly higher absorbance in the UV−vis spectrum than cymantrene. The absorbance coefficient ϵ of **3** in *n*-hexane is 1700 L mol^{-1} cm^{-1} (λ_{max} = 298 nm), and the corresponding transition in cymantrene at 328 nm has a coefficient of 1150 L mol^{-1} cm^{-1}.[21] Therefore, the reactivity enhancement of triphosphacymantrene **3** cannot be caused by this effect. Additionally, the photolysis of carbacyclic cymantrenes is very efficient, as the quantum yields are about 0.8.[20] We believe, therefore, that the photochemical reaction pathway is accompanied by a thermal one, too. In agreement with this assumption **3** reacts at slightly elevated temperatures such as 70 °C to form the monoisonitrile complex **11** in a few hours. No such reactions are known for cymantrene, but several unsuccessful attempts have been reported.[27] There is only one exception, as Coville managed to react cymantrene at high temperatures with isonitriles by utilizing PdO as a catalyst, but long reactions times are required.[28]

The thermal reaction of (η^5-*t*-$Bu_2C_2P_3$)$Co(CO)_2$ (**4**) with cyclohexylisonitrile is accelerated as well. At room temperature the disubstituted complex **9** is formed in good yield, whereas only the monosubstituted derivative of $CpCo(CO)_2$ can be made this way. To replace both CO ligands, the more reactive phenylisonitrile and elevated temperatures are required.[11]

While for the cobalt complex **4** the reactivity is just accelerated, triphosphacymantrene **3** exhibits a new kind of reactivity. A thermally induced dissociative pathway for **3** can be ruled out, as the CO stretching frequencies of **3** and cymantrene are almost identical.[5,29]

On the other hand, the high reactivity of **3** may be due to an associative reaction mechanism in combination with a ring slippage of the triphospholyl ring and the formation of a manganese-coordinated phosphaallyl or diphosphaallyl substructure.

A similar mechanism has been stated by Basolo for azacymantrene derivatives with a π-coordinated pyrrol ligand, which undergo thermally initiated carbonyl exchange reactions at 130 °C. In the solid state the pyrrol ligand is slipped toward the nitrogen atom by about 6 pm. This has been taken as evidence for a ring slippage toward an η^3-complexing mode of the ligand.[30]

For a diphospholyl ligand an η^3-coordination has been already observed,[3] and in the case of iron as central metal, coordinated phosphaallyl and diphosphaallyl ligand substructures are regularly associated with small valence electron counts.[31] This should be in principle possible for the neighboring element manganese as well. The enhanced reactivity of cobalt complex **4** may be due to an easier ring slippage as well. Unlike cymantrene, cyclopentadienylcobalt dicarbonyl already reacts by an associative mechanism;[24] thus the lesser pronounced differences between $Cp(CO)_2Co$ and its triphospha analogue **4** can be explained with the same picture.

Conclusions

Triphospholylmetal carbonyl complexes such as **3** or **4** undergo effective carbonyl exchange reactions under both photochemical and thermal conditions. If compared with their carbacyclic counterparts, equivalent products are formed photochemically, but the reaction times are significantly shortened.

Under thermal reaction conditions the reactions proceed at much lower temperatures than observed for cyclopentadienyl complexes. While cymantrene is inert toward thermal carbonyl exchange, its triphospha analogue **3** reacts under relatively mild conditions. This behavior points to an additional reaction pathway. An associative substitution mechanism in conjunction with a ring slippage of the triphospholyl ligand is postulated.

Experimental Section

General Considerations. All experiments were conducted under nitrogen by using standard Schlenk and cannula techniques. Solvents were dried according to described procedures[32] and used freshly distilled from the drying agent. NMR solvents have been purchased from Sigma-Aldrich. [D_8] toluene and [D_6] benzene were dried with potassium benzophenone, distilled, and stored over molecular sieves. $CDCl_3$ was degassed and stored over molecular sieves. Cyclohexylisonitrile was purchased from Fluka Chemie AG and used without further purification. Triphenylphosphane was purchased from MERCK-Schuchardt and was recrystallized from methylcyclohexane. Dicobaltoctacarbonyl-, trimethyl-, and triethylphosphane have been prepared using standard methods. Triphosphacymantrene (**3**) and 1-triorganylstannyl-3,5-di(*tert*-butyl)-1,2,4-triphosphole (**2**) were prepared as described before.[5,12]

(η^5-*t*-$Bu_2C_2P_3$)$(CO)_2$Co (4). At 0 °C 1 g (2.92 mmol) of $Co_2(CO)_8$ in 40 mL of *n*-hexane is mixed with 1.63 g (2.8 mmol) of (η^1-*t*-$Bu_2C_2P_3$)($SnPh_3$) (**2**) in 70 mL of *n*-hexane. The solution is allowed to reach room temperature overnight. A ^{31}P NMR spectrum shows **4** as the only phosphorus-containing species. The solution is concentrated in vacuo and distilled in a Kugelrohr apparatus in an oil pump vacuum. (η^5-*t*-$Bu_2C_2P_3$)$(CO)_2$Co (**4**) (0.189 g, 0.500 mmol, 19.5%) is obtained at 150 °C as a red liquid, which solidifies at ca. −10 °C.

(26) Breque, A.; Mathey, F. *J. Organomet. Chem.* **1978**, *144*, C9−C11.
(27) Strohmeier, W.; Barbeau, C. *Z. Naturforsch. B* **1962**, *17*, 848−849. Angelici, R. J.; Loewen, W. *Inorg. Chem.* **1967**, *6*, 682−686.
(28) Harris, G. W.; Boeyens, J. C. A.; Coville, N. J. *J. Organomet. Chem.* **1983**, *255*, 87−94.
(29) Shen, L. M. C.; Long, G. G.; Moreland, C. G. *J. Organomet. Chem.* **1966**, *5*, 362−369.
(30) Ji, L.-N.; Kerschner, D. L.; Basalo, F. *J. Organomet. Chem.* **1985**, *296*, 83−94. Kerschner, D. L.; Basalo, F.; Rheingold, A. L. *Organometallics* **1987**, *6*, 196−198.
(31) Hu, D.; Schäufele, H.; Pritzkow, H.; Zenneck, U. *Angew. Chem.* **1989**, *101*, 929−931. Driess, M.; Hu, D.; Schäufele, H.; Pritzkow, H.; Regitz, M.; Rösch, W.; Zenneck, U. *J. Organomet. Chem.* **1987**, *334*, C35−C38.
(32) Perrin, D. D.; Armarego, W. L. F. *Purification of Laboratory Chemicals*, 3rd ed.; Butterworth-Heinemann: Oxford, 1988.

Spectroscopic Data for 4. ^{1}H NMR (269.7 MHz, $CDCl_3$, rt): δ 1.37 (br, 18H, C(CH_3)$_3$). ^{31}P{^{1}H} NMR (161.7 MHz, $CDCl_3$, 20.4 °C): [AB_2] spin system, δ 121.93 (t, $^2J(^{31}P,^{31}P)$ = 42 Hz, 1P, *P*(A)), 118.99 (d, $^2J(^{31}P,^{31}P)$ = 42 Hz, 2P, *P*(B)). ^{13}C{^{1}H} NMR (100.4 MHz, $CDCl_3$, 26.4 °C): δ 200.46 (s, *C*O), 167.08 (dpt, $^1J(^{31}P,^{13}C)$ = 81 Hz, $\Sigma\,^1J(^{31}P,^{13}C) + {}^2J(^{31}P,^{13}C)$ = 104 Hz, C_{ring}), 39.17 (dpt, $^2J(^{31}P,^{13}C)$ = 17 Hz, $\Sigma^2J(^{31}P,^{13}C) + {}^3J(^{31}P,^{13}C)$ = 12 Hz, *C*(CH$_3$)$_3$), 36.05 (not res., C(*C*H$_3$)$_3$). IR (*n*-hexane): ν(CO) 2035, 1990 cm^{-1}. Mp: ca. −10 °C.

(η^5-*t*-$Bu_2C_2P_3$)(CO){$P(CH_2CH_3)_3$}Co (5). At 0 °C 79 mg (0.228 mmol) of (η^5-*t*-$Bu_2C_2P_3$)(CO)$_2$Co (**4**) and 0.5 mL of triethylphosphane (0.4 g, 3.4 mmol) in 80 mL of *n*-hexane are irradiated in a Pyrex glass apparatus for 10 min with a 125 W high-pressure mercury lamp. The color changes to deep red. The solution is filtered, the solvent removed in vacuo, and the residue chromatographed on SiO_2/5% H_2O with *n*-hexane as eluent. The main red fraction is collected to get 51 mg (0.117 mmol, 51.4%) of (η^5-*t*-$Bu_2C_2P_3$)(CO){$P(CH_2CH_3)_3$}Co (**5**) as a red oil.

Spectroscopic Data for 5. ^{1}H NMR (269.7 MHz, $CDCl_3$, rt): δ 1.80 (dq, $^2J(^1H,^{31}P)$ = 8.8 Hz, $^3J(^1H,^1H)$ = 7.5 Hz, 6H, CH_2), 1.39 (s, 18H, C(CH_3)), 1.10 (dt, $^3J(^1H,^{31}P)$ = 16.0 Hz, $^3J(^1H,^1H)$ = 7.5 Hz, 9H, CH_3). ^{31}P{^{1}H} NMR (161.7 MHz, $CDCl_3$, 20.1 °C): [A_2BX] spin system, δ 44.8 (br, 1P, *P*Et$_3$), 81.1 (dt, $^2J(^{31}P,^{31}P)$ = 39.4 Hz, $^2J(^{31}P,^{31}P)$ = 8.6 Hz, 1P, P_{ring}), 83.57 (d, $^2J(^{31}P,^{31}P)$ = 39.4 Hz, 2P, P_{ring}). ^{13}C{^{1}H} NMR (67.83 MHz, $CDCl_3$, rt): δ 204.0 (s, *C*O), 164.8 (ddpt, $^1J(^{13}C,^{31}P)$ = 77.2 Hz, $\Sigma^1J(^{13}C,^{31}P) + {}^2J(^{13}C,^{31}P)$ = 104.4 Hz, $^2J(^{13}C,^{31}P)$ = 2.9 Hz, C_{ring}), 38.5 (dpt, $^2J(^{13}C,^{31}P)$ = 18.0 Hz, $\Sigma^2J(^{13}C,^{31}P) + {}^3J(^{13}C,^{31}P)$ = 11.6 Hz, *C*(CH$_3$)$_3$), 36.6 (dpt, $^3J(^{13}C,^{31}P)$ = 8 Hz, $\sum^3J(^{13}C,^{31}P) + {}^4J(^{13}C,^{31}P)$ = 8 Hz, C(*C*H$_3$)$_3$), 23.7 (d, $^1J(^{13}C,^{31}P)$ = 29 Hz, *C*H$_2$), 8.3 (s, *C*H$_3$). IR (*n*-hexane): ν(CO) 1941 cm^{-1}. MS (FD$^+$, *n*-hexane): *m*/*z* (%) 436 (100) [M]$^+$.

(η^5-*t*-$Bu_2C_2P_3$)(CO){$P(C_6H_5)_3$}Co (6). At −15 °C 72 mg (0.208 mmol) of (η^5-*t*-$Bu_2C_2P_3$)(CO)$_2$Co (**4**) and 260 mg (0.99 mmol) of triphenylphosphane in 120 mL of *n*-hexane are irradiated in a Pyrex glass apparatus for 15 min with a 125 W high-pressure mercury lamp. The color changes to bordeaux red. The solution is filtered, the solvent removed in vacuo, and the residue chromatographed on SiO_2/5% H_2O with a 4:1 mixture of *n*-hexane and toluene as eluent. The main bordeaux red fraction is collected, and the solvents are removed in vacuo again. The product is recrystallized from *n*-hexane at 4 °C to yield 83 mg (0.143 mmol, 69%) of (η^5-*t*-$Bu_2C_2P_3$)(CO){$P(C_6H_5)_3$}Co (**6**) as deep red crystals.

Spectroscopic Data for 6. ^{1}H NMR (269.7 MHz, $CDCl_3$, rt): δ 1.40 (s, 18H, CH_3), 7.37 (m, 9H, *o*- and *p*-Ph-*H*), 7.61 (m, 6H, *m*-Ph-*H*). ^{31}P{^{1}H} NMR (161.7 MHz, $CDCl_3$, 24.9 °C): [A_2-BX] spin system, δ 57.1 (br, 1P, *P*(C_5H_6)$_3$), 75.8 (dt, $^2J(^{31}P,^{31}P)$ = 10.8 Hz, $^2J(^{31}P,^{31}P)$ = 36.2 Hz, 1P, P_{ring}), 97.2 (d, $^2J(^{31}P,^{31}P)$ = 36.2 Hz, 2P, P_{ring}). ^{13}C{^{1}H} NMR (67.83 MHz, $CDCl_3$, rt): δ 36.61 (dpt, $^3J(^{31}P,^{13}C)$ = 8.8 Hz, $\sum^3J(^{31}P,^{13}C) + {}^4J(^{31}P,^{13}C)$ = 8.8 Hz, *C*H$_3$), 39.00 (dpt, $^2J(^{31}P,^{13}C)$ = 18.0 Hz, $\Sigma^2J(^{31}P,^{13}C) + {}^3J(^{31}P,^{13}C)$ = 11.6 Hz, *C*(CH$_3$)$_3$), 127.89 (d, $^3J(^{31}P,^{13}C)$ = 10.4 Hz, *m*-Ph-*C*), 129.99 (d, $^4J(^{31}P,^{13}C)$ = 2.6 Hz, *p*-Ph-*C*), 134.00 (d, $^2J(^{31}P,^{13}C)$ = 10.9 Hz, *o*-Ph-*C*), 137.03 (d, $^1J(^{31}P,^{13}C)$ = 46.11 Hz, *i*-Ph-*C*), 166.32 (ddpt, $^2J(^{31}P(PPh_3),^{13}C)$ = 3.3 Hz, $^1J(^{31}P,^{13}C)$ = 76.3 Hz, $\Sigma^1J(^{31}P,^{13}C) + {}^2J(^{31}P,^{13}C)$ = 104.2 Hz, C_{ring}), 203 (s, *C*O). IR (*n*-hexane): ν(CO) 1953 cm^{-1}. MS (FD$^+$, CH_2Cl_2): *m*/*z* (%) 580 (100) [M]$^+$. Anal. Calcd for ($C_{29}H_{33}CoOP_4$): C 60.01, H 5.73. Found: C 60.10, H 6.04. Mp: 151 °C.

(η^5-*t*-$Bu_2C_2P_3$)(CO){$P(CH_3)_3$}$_2$Mn (7). A 0.124 g (0.335 mmol) sample of (η^5-*t*-$Bu_2C_2P_3$)(CO)$_3$Mn (**3**) and 4 mL (2.95 g, 38.8 mmol) of trimethylphosphane are irradiated in 60 mL of *n*-hexane in a Pyrex glass apparatus at −20 °C for 15 min with a 125 W high-pressure mercury lamp. The color changes from bright yellow to orange-red. All volatile substances are removed in vacuo, and the orange residue is chromatographed on SiO_2/5% H_2O with a 5:2 mixture of *n*-hexane and toluene. The main orange-red fraction is collected, and the solvent is removed in vacuo again. By crystallization from *n*-hexane at −18 °C 115 mg (0.247 mmol, 73.6%) of (η^5-*t*-$Bu_2C_2P_3$)(CO)-{$P(CH_3)_3$}$_2$Mn (**7**) are obtained as red crystals.

Spectroscopic Data for 7. ^{1}H NMR (399.65 MHz, $CDCl_3$, 21.6 °C): δ 1.36 (s, CH_3), 1.59 (s, CH_3). ^{1}H NMR (269.7 MHz, [D_8] toluene, −59.9 °C): δ 1.48−1.77 (m, 27H, P(CH_3)$_3$ and C(CH_3)$_3$)), 1.94 (s, 9H, C(CH_3)$_3$)). ^{31}P{^{1}H} NMR (161.7 MHz, [D_8] toluene, −59.9 °C): [ABCDE] spin system, δ 22.6 (d, $^2J(^{31}P,^{31}P)$ = 59 Hz, 1P, *P*(CH$_3$)$_3$), 28.2 (d, $^2J(^{31}P,^{31}P)$ = 59 Hz, 1P, *P*(CH$_3$)$_3$), 33.0 (dd, $^1J(^{31}P,^{31}P)$ = 423 Hz, $^2J(^{31}P,^{31}P)$ = 42 Hz, 1P, P_{ring}), 72.6 (dd, $^2J(^{31}P,^{31}P)$ = 42 Hz, $^2J(^{31}P,^{31}P)$ = 42 Hz, 1P, P_{ring}), 85.3 (dd, $^1J(^{31}P,^{31}P)$ = 423 Hz, $^2J(^{31}P,^{31}P)$ = 42 Hz, 1P, P_{ring}). ^{31}P{^{1}H} NMR (161.7 MHz, [D_8] toluene, +90.0 °C): [AB_2C_2] spin system, δ 24.0 (s, 2P, *P*(CH$_3$)$_3$), 62 (br, 2P, P_{ring}), 77.4 (t, $^2J(^{31}P,^{31}P)$ = 42 Hz, 1P, P_{ring}). ^{13}C{^{1}H} NMR (100.40 MHz, $CDCl_3$, 22.6 °C): δ 25.1 (br, P(*C*H$_3$)$_3$), 36.1 (br, C(*C*H$_3$)$_3$), 37.0 (br, *C*(CH$_3$)$_3$), 232 (s, *C*O). ^{13}C{^{1}H} NMR (100.40 MHz, [D_8] toluene, 0.0 °C): δ 22.8 (br, P(*C*H$_3$)$_3$), 24.0 (br, P(*C*H$_3$)$_3$), 34.9 (br, C(*C*H$_3$)$_3$), 35.7 (br, *C*(CH$_3$)$_3$) 230.5 (m, *C*O). ^{13}C{^{1}H} NMR (100.40 MHz, [D_8] toluene, −59,9 °C): δ 23.8 (P(*C*H$_3$)$_3$), 25.5 (P(*C*H$_3$)$_3$), 36.2 (C(*C*H$_3$)$_3$), 36.6 (C(*C*H$_3$)$_3$), 36.9 (dd, $^2J(^{13}C,^{31}P)$ = 17.6 Hz, $^2J(^{13}C,^{31}P)$ = 17.6 Hz, *C*(CH$_3$)$_3$), 38.0 (dd, $^2J(^{13}C,^{31}P)$ = 16.6 Hz, $^2J(^{13}C,^{31}P)$ = 16.6 Hz, *C*(CH$_3$)$_3$), 144.8 (dd, $^1J(^{13}C,^{31}P)$ = 88.4 Hz, $^1J(^{13}C,^{31}P)$ = 70.8 Hz, C_{ring}) 149.6 (dd, $^1J(^{13}C,^{31}P)$ = 90.4 Hz, $^1J(^{13}C,^{31}P)$ = 73.5 Hz, C_{ring}) 232.5 (dd, $^2J(^{13}C,^{31}P(PMe_3))$ = 32 Hz, $^2J(^{13}C,^{31}P(PMe_3))$ = 32 Hz, *C*O). Due to limited measurement time at low temperature, only part of the P−C splittings are resolved in ^{13}C NMR. IR (*n*-hexane): ν(CO) 1863 cm^{-1}. MS (FD$^+$, *n*-hexane): *m*/*z* (%) 467 (100) [M]$^+$. Anal. Calcd for ($C_{17}H_{36}MnOP_5$): C 43.79, H 7.78. Found: C 44.06, H 8.26. Mp: 132 °C.

{μ[1:1−5-η-*t*-$Bu_2C_2P_3$](CO)$_2$Mn}$_2$ (8a and 8b). A 159 mg (0.430 mmol) sample of (η^5-*t*-$Bu_2C_2P_3$)(CO)$_3$Mn (**3**) in 180 mL of *n*-hexane is irradiated in a Pyrex glass apparatus at 0 °C for 10 min with a 125 W high-pressure mercury lamp. The solution is filtered, and the solvent is removed in vacuo. The residue is chromatographed on SiO_2/5% H_2O with a 1:1 mixture of *n*-hexane and toluene as eluent to get a deep red fraction. The solvent is removed in vacuo, and the orange-red solid is recrystallized from *n*-hexane at −18 °C to yield 88 mg (0.128 mmol, 60%) of a mixture of the *rac* and *meso* complexes {μ[1:1−5-η-*t*-$Bu_2C_2P_3$](CO)$_2$Mn}$_2$ (**8a** and **8b**) as a red microcrystalline solid.

Spectroscopic Data for an Approximately 1:2 Mixture of 8a and 8b. ^{1}H NMR (269.7 MHz, $CDCl_3$, rt): **8a**: δ 1.41 (s, 18H, CH_3), 1.23 (s, 18H, CH_3); **8b**: 1.61 (s, 18H, CH_3), 1.24 (s, 18H, CH_3). ^{31}P{^{1}H} NMR (161.70 MHz, $CDCl_3$, 23 °C): **8a**: [AA′XX′YY′] spin system, δ 95.64 (m, 2P, *P*(A)), ∼78 (m, 2P, *P*(X)), 61.73 (m, 2P, *P*(Y)); **8b**: [ABC]$_2$ spin system, δ 77.46 (br, dd, $^1J(^{31}P,^{31}P)$ = 424.5 Hz, $^2J(^{31}P,^{31}P)$ = 42.1 Hz, 2P, *P*(A)), 79.98 (dd, $^1J(^{31}P(2),^{31}P(3))$ = 424.5 Hz, $^2J(^{31}P,^{31}P)$ = 38.8 Hz, 2P, *P*(B)), 72.96 (dd, $^2J(^{31}P,^{31}P)$ = 42.1 Hz, $^2J(^{31}P,^{31}P)$ = 38.8 Hz, 2P, *P*(C)). IR (*n*-hexane): ν(CO) 1962, 1930 cm^{-1}. MS (FD$^+$, *n*-hexane): *m*/*z* (%) 685 (100) [M]$^+$. Anal. Calcd for ($C_{24}H_{36}$-$Mn_2O_4P_6$): C 42.13, H 5.30. Found: C 42.27, 5.61.

(η^5-*t*-$Bu_2C_2P_3$)(CNCy)$_2$Co (9) and (η^5-*t*-$Bu_2C_2P_3$)(CO)-(CNCy)Co (10). At −60 °C 0.072 g (0.208 mmol) of (η^5-*t*-$Bu_2C_2P_3$)(CO)$_2$Co (**4**) in 20 mL of *n*-hexane is reacted with 6 mL of a cyclohexylisonitrile solution (0.045 g, 0.41 mmol isonitrile in THF/*n*-hexane). The solution is allowed to warm to room temperature and is stirred for an additional 1.5 h. The solvent and all volatile substances are removed in vacuo. The residue is redissolved in *n*-hexane and filtered to get an orange-red solution, part of the solvent is removed in vacuo, and the resulting solution is chromatographed on SiO_2/5% H_2O with a 3:1 mixture of *n*-hexane and toluene as eluent. Two fractions are collected. The first orange one gives 8 mg (0.019 mmol, 9%) of (η^5-*t*-$Bu_2C_2P_3$)(CNCy)(CO)Co (**10**) as a red oil. The second fraction results in a orange-brown solid, which is recrystallized from *n*-hexane at −18 °C to yield 81 mg (0.159

mmol, 77%) of (η^5-*t*-$Bu_2C_2P_3$)$(CNCy)_2Co$ (**9**) as dark red needles and brownish yellow plates.

Spectroscopic Data for 9. ^1H NMR (399.65 MHz, C_6D_6, 22.3 °C): δ 3.18 (m, 2H, α-Cy-*H*), 1.75 (s, 18H, CH_3), ∼1.5 (m, 8H, Cy-*H*), ∼1.4 (m, 4H, Cy-*H*), ∼1.1 (m, 4H, Cy-*H*), ∼1.0 (m, 4H, Cy-*H*). $^{31}P\{^1H\}$ NMR (161.7 MHz, C_6D_6, 22.6 °C): [A_2B] spin system, δ 97.79 (d, $^2J(^{31}P,^{31}P) = 47.7$ Hz, 2P, *P*(A)), 103.66 (t, $^2J(^{31}P,^{31}P) = 47.4$ Hz, 1P, *P*(B)). $^{13}C\{^1H\}$ NMR (100.4 MHz, C_6D_6, 21.8 °C): δ 158.54 (s, *C*N), 149.08 (dpt, $^1J(^{31}P,^{13}C) = 76.9$ Hz, $\sum^1J(^{31}P,^{13}C) + {}^2J(^{31}P,^{13}C) = 100.8$ Hz, C_{ring}), 54.75 (s, Cy-(α-*C*)), 39.07 (dpt, $^2J(^{31}P,^{13}C) = 18.2$ Hz, $\sum^2J(^{31}P,^{13}C) + {}^3J(^{31}P,^{13}C) = 13.2$ Hz, *C*$(CH_3)_3$), 36.39 (not res., C(*C*$H_3)_3$), 33.22 (s, Cy (*β*- or *γ*- or *δ*-*C*)), 25.38 (s, Cy (*β*- or *γ*- or *δ*-*C*)), 23.29 (s, Cy (*β*- or *γ*- or *δ*-*C*)). IR (*n*-hexane): *ν*(CN) 2120 cm^{-1}. MS (FD^+, CH_2Cl_2): *m*/*z* (%) 508 (100) $[M]^+$. Anal. Calcd for ($C_{24}H_{40}CoN_2P_3$): C 56.70, N 5.51, H 7.93. Found: C 57.09, N 5.36, H 8.24. Mp: decomposition without melting at ca. 120 °C.

Spectroscopic Data for 10. ^1H NMR (269.7 MHz, C_6D_6, rt): δ 2.72 (m, 1H, α-Cy-*H*), 1.46 (s, 18H, CH_3), 0.6−1.4 (m, 10H, Cy-*H*). $^{31}P\{^1H\}$ NMR (161.7 MHz, C_6D_6, 26.2 °C): [AB_2] spin system, δ 112.38 (t, $^2J(^{31}P,^{31}P) = 45.8$ Hz, 1P, *P*(A)), 111.58 (d, $^2J(^{31}P,^{31}P) = 45.8$ Hz, 2P, *P*(B)); the chemical shifts and coupling constants have been obtained by using the analytic solution for an [AB_2] spin system. $^{13}C\{^1H\}$ NMR (100.4 MHz, C_6D_6, 25.0 °C): δ 158.29 (dpt, $^1J(^{31}P,^{13}C) = 88.8$ Hz, $\sum^1J(^{31}P,^{13}C) + {}^2J(^{31}P,^{13}C) = 118.4$ Hz, C_{ring}), 54.95 (s, Cy (α-*C*)), 39.01 (dpt, $^2J(^{31}P,^{13}C) = 17.0$ Hz, $\sum^2J(^{31}P,^{13}C) + {}^3J(^{31}P,^{13}C) = 13.6$ Hz, *C*$(CH_3)_3$), 36.06 (not res., C(*C*$H_3)_3$), 32.38 (s, Cy (*β*- or *γ*- or *δ*-*C*)), 24.76 (s, Cy (*β*- or *γ*- or *δ*-*C*)), 22.92 (s, Cy (*β*- or *γ*- or *δ*-*C*)); due to the small amounts of **10**, the signals of the isonitrile and carbonyl *C* atoms could not be detected. IR (*n*-hexane): *ν*(CO) 1978 cm^{-1}, *ν*(CN) 2135 cm^{-1}. MS (FD^+, *n*-hexane): *m*/*z* (%) 427 (100) $[M]^+$.

(η^5-*t*-$Bu_2C_2P_3$)$(CNCy)(CO)_2Mn$ (11). A 108 mg (0.292 mmol) sample of (η^5-^{t}$Bu_2C_2P_3$)$(CO)_3Mn$ (**3**) and 1 mL of cyclohexylisonitrile (0.88 g, 8.06 mmol) in 80 mL of *n*-hexane are refluxed for 3 h. The bright yellow color changes to orange. According to IR control, no (η^5-*t*-$Bu_2C_2P_3$)$(CO)_3Mn$ (**3**) is left over. The solution is allowed to cool to room temperature, all volatile substances are removed in vacuo, and the residue is chromatographed on SiO_2/5% H_2O with *n*-hexane as eluent. The first fraction is collected to yield 69 mg (0.153 mmol, 52.4%) of (η^5-^{t}$Bu_2C_2P_3$)$(CO)_2$(CN−Cy)Mn (**11**) as an orange to red liquid.

Spectroscopic Data for 11. ^1H NMR (399.65 MHz, C_6D_6, 21.3 °C): δ 2.87 (m, 1H, α-Cy-*H*), 1.36 (s, 18H, CH_3), 0.5−1.4 (m, 10H, Cy-*H*). $^{31}P\{^1H\}$ NMR (161.7 MHz, C_6D_6, 22.5 °C): [AB_2] spin system, δ 103.64 (m, 3P). $^{13}C\{^1H\}$ NMR (100.40 MHz, [D_8] toluene, rt): δ 169.5 (s, CN), 157.06, 156.32, 156.12, 156.12, 155.51, 155.17, 154.44 (each s, X-part of an AB_2X spectrum (A, B = ^{31}P, X = ^{13}C), C_{ring}), 58.07 (s, Cy (α-*C*)), 38.91, 38.82, 38.78, 38.69, 38.64, 38.64, 38.55, 38.46 (each s, X-part of an AB_2X spectrum (A, B = ^{31}P, X = ^{13}C), *C*$(CH_3)_3$), 36.57, 36.50, 36.50, 36.45, 36.42, 36.42, 36.38, 36.32 (each s, X-part of an AB_2X spectrum (A, B = ^{31}P, X = ^{13}C), C(*C*$H_3)_3$), 36.85 (s, Cy (*β*-*C*)), 27.93 (s, Cy (*γ*-*C*)), 26.04 (s, Cy (*δ*-*C*)). IR (*n*-hexane): *ν*(CN) 2118, *ν*(CO) 1968, 1927 cm^{-1}. MS (FD^+, *n*-hexane): *m*/*z* (%) 451 (100) $[M]^+$.

Crystal Structure Determination of 9. Crystal data were collected on a Bruker AXS SMART 1000 diffractometer with CCD area detector (Mo Kα radiation, graphite monochromator, $\lambda = 0.71073$ Å) using the SMART software.[33] The reflection intensities were integrated using SAINT[33] and corrected for absorption using SADABS.[34] The structures were solved by direct methods and refined by full-matrix least-squares procedures against F^2 with all reflections using SHELXTL-programs.[35] All non-hydrogen atoms were refined anisotropically. All hydrogen atoms were located in difference Fourier maps and refined isotropically. Crystal data and experimental details are listed in Table 4.

Crystal Structure Determinations of 4, 6, 7, 8a, and 8b. Data were collected on a Siemens P4 (**4**, **7**, **8a**, **8b**) or a Nicolet R3m/V diffractometer (**6**) using Mo Kα radiation (λ = 0.71073 Å, graphite monochromator). Reflection intensities were corrected for Lorentz and polarization effects. An absorption correction has been applied using *ψ*-scans (**4**, **7**, **8a**, **8b**),[35] while for **6** absorption effects have been neglected. The structures were solved by direct methods and refined by full-matrix least-squares procedures against F^2 with all reflections using SHELXTL NT 5.1.[35] All non-hydrogen atoms were refined anisotropically. The hydrogen atoms were located in difference Fourier maps and refined with a fixed common isotropic displacement parameter. Crystal data and experimental details are listed in Tables 1, 4, and 6.

Acknowledgment. This work was supported by the Deutsche Forschungsgemeinschaft and the Fonds der Chemischen Industrie. M.Z. is grateful for a scholarship by the DFG-Graduiertenkolleg Phosphorchemie als Bindeglied verschiedener chemischer Disziplinen, at the University of Kaiserslautern, Germany. We also thank Dr. M. Moll for the measurement of variable-temperature NMR spectra.

Supporting Information Available: Further details of the structure determination including tables of atomic coordinates, bond distances and angles, and thermal parameters. This material is available free of charge via the Internet at http://pubs.acs.org.

OM001068Q

(33) *SMART* and *SAINT, NT V5.0*, Area detector control and integration software; Bruker AXS: Madison, WI, 1999.
(34) Sheldrick, G. M. *SADABS, Program for scaling and correction of area detector data*; Göttingen, Germany, 1996.
(35) Sheldrick, G. M. *SHELXTL NT V5.1*, Bruker AXS: Madison, WI, 1999.